Optica Applicata, Vol. XLVII, No. 4, 2017
DOI: 10.5277/oa170402

Optical sizing of cement particles

MYKHAYLO P. GORSKY*, PETER P. MAKSIMYAK

Yuriy Fedkovych Chernivtsi National University, 2 Kotsjubynskyi St., Chernivtsi, Ukraine

*Corresponding author: mikegood@gmail.com

We represent the optical correlation technique of cement particle sizing based on the transverse coherency function measurement using a polarization transverse shearing interferometer. It is shown that a set of particles with random shapes and orientations produces a coherence function, which is the same as a function of the set of spherical particles. The proposed technique of experimental data processing decreases the dependence of the result on interferometer noise, emission source intensity fluctuations and differences in the refraction index of isolated cement particles. The described technique allows fast and high reliable determining of the size distribution function parameters for a set of cement particles.

Keywords: transverse coherence, polarization interferometer, cement, size distribution function.

1. Introduction

The size distribution function (SDF) of particles is an important concrete and cement characteristics. Different kinds and brands of cement differ by particle sizes. For physical and mathematical modeling of various processes, which occur during concrete hydration, studying its mechanical, optical and other properties, it is necessary to know the SDF of particles. Cement particle SDF size measurements are taken by different techniques, such as electrical zone sensing, sedimentation, scanning electron microscopy [1–5]. But these techniques are rather complicated and are not widely used. A standard technique consisting in measurements of cement particles remaining weight on the sieve while consecutive screening is performed from the biggest mesh aperture to the smallest. A widely used optical approach is a laser diffraction (LDF) technique [5]. It is based on the measurement of a diffraction angle during laser light scattering on the flow of particles which are weighted in air. Here we propose the optical correlation technique for determining the parameters of cement particles' SDF [6, 7].

It is known that optical properties, for different kinds of effects like scattering and so on, are mathematically calculated only for spherical, cylindrical and spheroid forms of particles [8–11]. Thus, for practical use, it is convenient to approximate cement particles like ones with spherical form [12]. For example, this approximation is used

in LDF [5]. But the obtained distribution depends essentially on incoming parameters for calculating. One of these parameters is a magnitude of a relative refraction index. The refraction index of cement materials is complex, but its real and imaginary parts are varying within the ranges $n = 1.5$ to $1.7, \chi = 0.003$ to 1.0 [1–5] for different particles. Usually, a specified refraction index magnitude is set for all particles, what causes the result distortions.

2. Measurement of coherence function using a polarization interferometer

At light scattering on the set of particles, the particle images can be projected into an observation plane. It is easy to analyze these images using the transverse coherence function (TCF) which is an autocorrelation of particles image. In the case when images are formed by coherent light, TCF magnitude for a specified displacement is determined by the interference pattern visibility, which for scalar optical fields is determined as

$$V = \frac{I_{\max} - I_{\min}}{I_{\max} + I_{\min}} \tag{1}$$

where $I_{\max}$ and $I_{\min}$ denotes maximal and minimal magnitudes of the resulting field at the interferometer output, respectively. Let us consider the formation of TCF [13] on autocorrelation of the image for a single particle (Fig. 1).

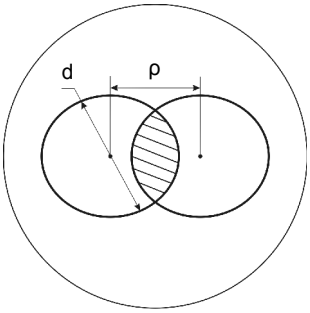

Fig. 1. Autocorrelation of a single particle image with diameter d when transverse displacement is ρ.

Let us denote the radiant flux through a unit area by ΔI. The particle image overlaps radiant flux in the beam. Then, at interference maximum, the radiant flux at the observation plane behind the particle image results from beam interference with zero phase difference and the total radiant flux is equal to $4\Delta I$. The radiant flux at the particle image area outside the overlapping image region equals ΔI. In the overlapped zone there would be a zero flux. The particle image zone square, outside the overlapped zone, is equal to $2[d^2\pi/4 - s_{\text{r}}(d, \rho)]$. If the observation zone square is bigger than the particle image square in ρ_{S} times, then the observation zone square, without particle

images, could be defined as $\rho_s d^2\pi/4 - 2[d^2\pi/4 - s_r(d, \rho)] - s_r(d, \rho)$. Then, maximum intensity for displacement ρ and particle diameter d can be written as

$$I_{\max}(\rho, d, \rho_s) = \begin{cases} \Delta I\left[d^2 \operatorname{acos}\left(\frac{\rho}{d}\right) + d^2\pi\left(\rho_s - \frac{3}{2}\right) - \rho\sqrt{d^2 - \rho^2}\right], & \rho \le d \\ \Delta I\, d^2\pi\left(\rho_s - \frac{3}{2}\right), & \rho > d \end{cases} \tag{2}$$

where ρ_s denotes value equal to the ratio between the observation field square and the particle image square. In the minimum intensity, the observation field would be the result of bundle interference with phase difference π, so the radiant flux outside the particle images and in the overlapped image zone would be equal to zero. The radiant flux in no overlapped zones of particle images is also equal to ΔI. Then, the minimum intensity in a transverse shearing interferometer for displacement ρ and for particle diameter d can be written as

$$I_{\min}(\rho, d) = \begin{cases} \Delta I\left[\frac{d^2\pi}{2} + \rho\sqrt{d^2 + \rho^2} - d^2 \operatorname{acos}\left(\frac{\rho}{d}\right)\right], & \rho \le d \\ \Delta I\,\frac{d^2\pi}{2}, & \rho > d \end{cases} \tag{3}$$

Then, the visibility dependence on transverse displacement, which is equal to TCF (denoted as $\Gamma_\perp$) can be written as

$$\frac{I_{\max} - I_{\min}}{I_{\max} + I_{\min}} = \Gamma_\perp(\rho, d, \rho_s)$$

$$= \begin{cases} \dfrac{d^2\pi(\rho_s - 2) - 2\rho\sqrt{d^2 - \rho^2} + 2d^2 \operatorname{acos}\left(\frac{\rho}{d}\right)}{d^2\pi(\rho_s - 1)}, & \rho \le d \\ \dfrac{\rho_s - 2}{\rho_s - 1}, & \rho > d \end{cases} \tag{4}$$

where ρ_s is equal to the ratio of the observation field square and the particle image square.

For the set of spherical particles with corresponding size distribution $p(d)$, the transverse coherence function is defined as [13]:

$$\Gamma_\perp^{\text{total}}(\rho, \rho_s) = \int_0^\infty p(d)\,\Gamma_\perp(\rho, d, \rho_s)\,\mathrm{d}d \tag{5}$$

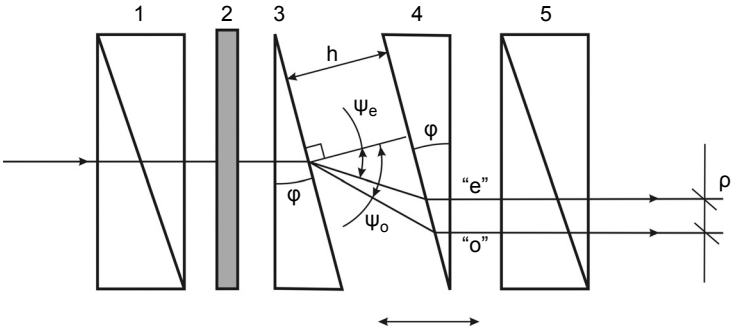

Fig. 2. Polarization interferometer. 1, 5 – crossed polarizers, 2 – sample, 3, 4 – wedges, "o", "e" – ordinary and extraordinary beam paths, respectively.

For displacement formation and TCF measurement, a polarization interferometer [13] can be used (Fig. 2). It consists of two identical wedges 3 and 4, which are placed between crossed polarizers 1 and 5 and form a plane-parallel plate. The main optical axes of wedges 3 and 4 are parallel and form 45° angle with the axes of maximal transmittance of polarizers 1 and 5. The sample 2 is placed between the polarizer 1 and the wedge 3. The ordinary "o" and extraordinary "e" beam paths are shown. Spatial separation of beams occurs at the output of the wedge 3.

Formation of the maximum or minimum of intensity of the resulting optical field at the interferometer output depends on the phase difference between ordinary "o" and extraordinary "e" beams.

In order to measure the global intensity of an image after polarization, the interferometer next setup can be used (Fig. 3). The beam from the laser 1, through the inverse telescopic system 2, illuminates the sample 3. The images of cement particles 3, through the polarization interferometer 4, using a micro-objective 5, are projected on a photodetector 6. The signal from a photodetector is recorded by a computer 7.

The longitudinal displacement between the beams in the interferometer causes the modulation of total field intensity. Also, the longitudinal displacement between two beams is linearly connected with the transverse displacement and it is convenient to

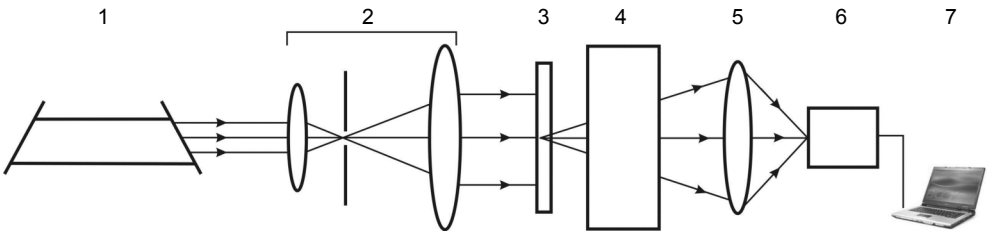

Fig. 3. Experimental arrangement: 1 – laser, 2 – inverse telescopic system with a diaphragm, 3 – sample, 4 – polarization interferometer, 5 – micro-objective, 6 – photodiode, 7 – computer.

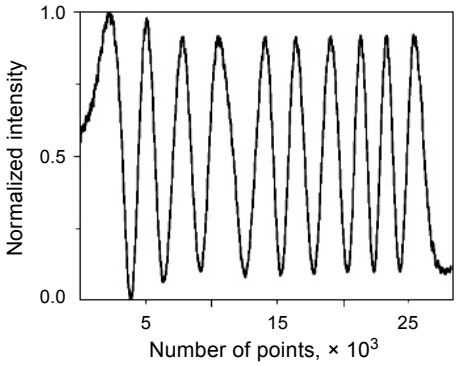

Fig. 4. Intensity modulation measured for longitudinal displacements of interferometer wedges.

use extreme magnitudes as markers (Fig. 4). The transverse displacement between extrema (maximum and minimum) is equal to $\lambda/2$.

3. Influence of a particle shape on the coherence function

In previous work [13] we found an analytical view of the function $p(d)$ for cement. Since cement particles were obtained as a result of grinding, the sizes of particles are random positive values. Such distributions are well approximated by the Rayleigh distribution (RD)

$$p_{\mathrm{r}}(d, \sigma) = \frac{d}{\sigma^2} \exp\left(-\frac{d^2}{2\sigma^2}\right) \tag{6}$$

where σ denotes the most probable value of a particle diameter.

Function (6) has only one parameter – σ which makes it suitable and convenient for a practical use.

All analytical calculations were performed for spherical particles and this raises the question about the accuracy of obtained results as far as real, random shape cement

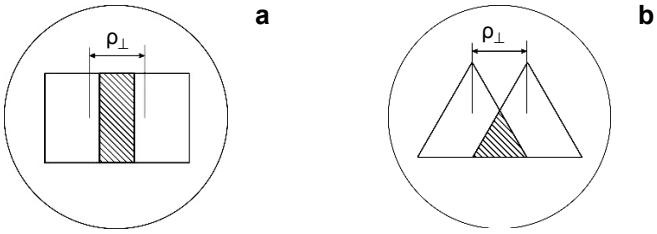

Fig. 5. Autocorrelation for a single particle of square (**a**) and triangle (**b**) shape with transverse displacement ρ.

particles are concerned. To answer this question, we performed the series of simulations for particles with square and triangle images (Fig. 5), which are close to real shapes of cement particles. The sizes of these square and triangle particles were chosen to have the same image projection area like for an appropriate spherical particle.

The result of simulation for single particles is shown in Fig. 6. As it can be seen, the coherence function for a single particle (Fig. 6) differs significantly for particles

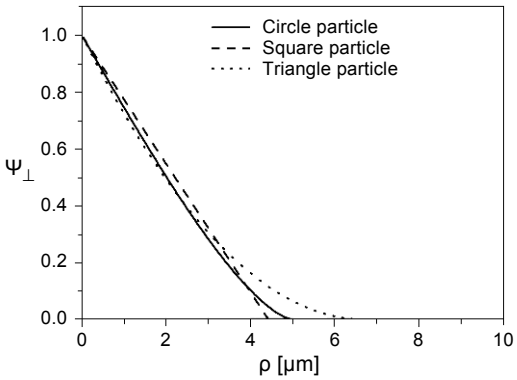

Fig. 6. TCF for single particles of circle, square and triangle shapes.

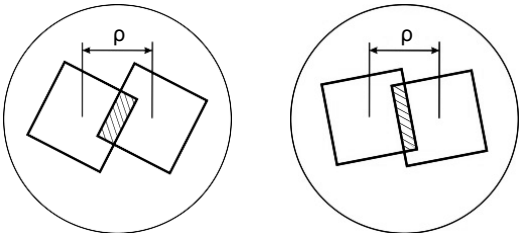

Fig. 7. Example of random orientation overlays of square particle images.

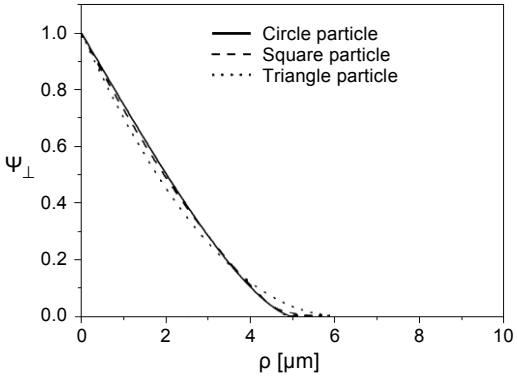

Fig. 8. TCF for the set of particles with uniform random orientations. Each triangle and square particle has an area which is equal to the area of a circle with the diameter of 5 μm.

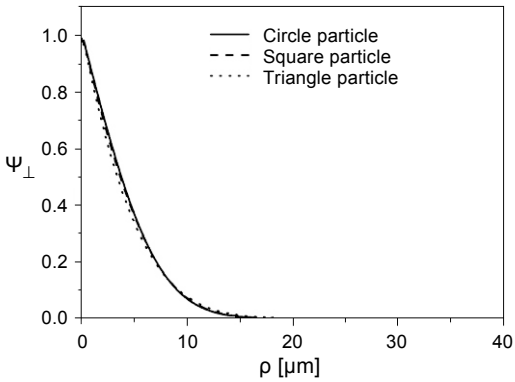

Fig. 9. TCF for the set of particles with uniform random orientations and the Rayleigh SDF with the most probable size 5 μm. Each triangle and square particle has an area equal to the area of a circle with the diameter of 5 μm.

with different shapes. But this difference vanishes if we add random orientations (Fig. 7) and specified distribution by sizes.

Figure 8 shows the coherence function for the set of particles with uniformly distributed random orientations.

Figure 9 shows the TCF for the set of particles with uniformly distributed random orientations and the Rayleigh SDF (6). The difference between TCFs is less than 3%.

Simulation showed that, although for a single particle it is not possible to consider random shaped particles as spheres, when we have a set of particles with random orientations and RD by sizes – TCF is almost the same like for an appropriate set of spherical particles.

4. Experimental results

Measurements were conducted for samples with a large and small concentration of cement particles. Samples were obtained by using a suspension of cement particles and ethanol. Then, the suspension was evaporated on a glass plate. By small concentration we meant the case when the distance between particles on a glass plate is bigger than the size of the biggest particle. Large concentration means that the distance is equal or less than the size of the biggest particle.

After measurements, in a setup, shown in Fig. 3, and using obtained extreme values, the parameters definition of Eq. (6) was taken from the condition of a minimum of mean square deviation between theoretical values of the transversal coherence function and experimentally obtained ones (Fig. 10).

Each experimental measurement brings information about the distribution of particles, which are situated at the observation field. That is why, to receive information on a whole cement particle SDF on a sample, we conducted measurements for different parts of the sample. The analysis of microscopic cement sample images shows that in different parts of the sample the most probable particle size varies in limits from 4

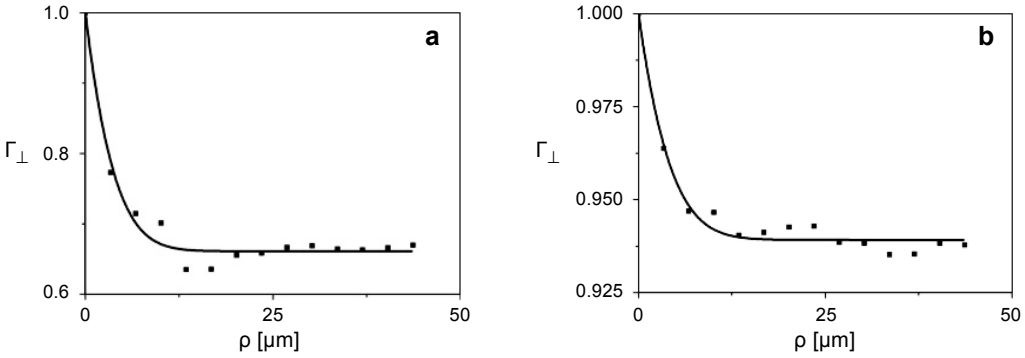

Fig. 10. Experimentally obtained coherence function (dots) and theoretical graph, obtained by the least -squares technique (line), for samples with large (**a**) and small (**b**) concentration of particles.

to 8 μm. There were conducted 10 measurements of samples with large and 10 with small concentration of particles. From the obtained experimental data, the function (5) parameters and ρ_s were found.

Processing of the obtained results gives us such confidence intervals with the confidence level $P = 0.95$: for samples with high concentration $\sigma = 3.9$ to 7.7 μm, and for samples with low concentration $\sigma = 3.7$ to 9.0 μm.

5. Conclusion

There were conducted 10 measurements of samples with a large and 10 with a small concentration of particles. Processing of the obtained results gives us such confidence intervals with level $P = 0.95$: for samples with high concentration $\sigma = 3.9$ to 7.7 μm, and for samples with low concentration $\sigma = 3.7$ to 9.0 μm. Average experimental values of the most probable cement particle size ($\sigma = 5.6$ μm for samples with high and $\sigma = 6.3$ μm for samples with low concentration of particles) correspond to values obtained for this cement by the sieve technique. The calculation technique developed by us decreases the calculated coherence function dependence on interferometer noise, emission source intensity fluctuations and different cement particles overlapping the image effect. Also, it has been shown that the coherence function for a set of randomly oriented particles with random sizes and shapes can be replaced with the function for spherical particles without the loss of accuracy.

References

[1] GORSKIY V.F., *Plugging Materials and Solutions. Handbook*, Oblpoligrafvydav, Chernivtsi, 2006, (in Ukrainian).

[2] LEE F.M., *The Chemistry of Cement and Concrete*, 3rd Ed., Chemical Publishing Company, 1971.

[3] RAMACHANDRAN V.S., BEAUDOIN J.J., *Handbook of Analytical Techniques in Concrete Science and Technology: Principles, Techniques and Applications*, William Andrew Inc., 2001.

[4] BULATOV A.I., DANYUSHEVSKIY V.S., *Plugging Materials Reference Manual*, Nadra, Moscow, 1987, (in Russian).

[5] FERRARIS C., HACKLEY V., AVILÉS A., *Measurement of particle size distribution in Portland cement powder: analysis of ASTM round robin studies*, Cement, Concrete and Aggregates **26**(2), 2004, pp. 1–11.

[6] ANGELSKY O.V., MAKSIMYAK P.P., *Optical correlation method for studying disperse media*, Applied Optics **32**(30), 1993, pp. 6137–6141.

[7] MAKSIMYAK P.P., ANGELSKY O.V., *An optical correlation method for measuring particle size and concentration*, Proceedings of IC Mechatronics 2000, Warsaw, Poland, 2000, pp. 466–468.

[8] ISHIMARU A., *Wave Propagation and Scattering in Random Media*. Vols. 1, 2, Academic Press, New York, 1978.

[9] ANGEL'SKIĬ O.V., USHENKO A.G., ARKHELYUK A.D., ERMOLENKO S.B., BURKOVETS D.N., USHENKO YU.A., *Laser polarimetry of pathological changes in biotissues*, Optics and Spectroscopy (Optika i Spektroskopiya) **89**(6), 2000, pp. 973–978.

[10] ANGELSKY O.V., TOMKA YU.YA., USHENKO A.G., USHENKO YE.G., YERMOLENKO S.B., USHENKO YU.A., *2-D tomography of biotissue images in pre-clinic diagnostics of their pre-cancer states*, Proceedings of SPIE **5972**, 2005, article ID 59720N.

[11] BORN M., WOLF E., *Principles of Optics*, Cambridge University Press, New York, 1999.

[12] GORSKY M.P., MAKSIMYAK P.P., MAKSIMYAK A.P., *Studies of light backscattering at concrete during its hydration*, Ukrainian Journal of Physical Optics **10**(3), 2009, pp. 134–149.

[13] GORSKY M.P., MAKSIMYAK P.P., MAKSIMYAK A.P., *Optical correlation technique for cement particle size measurements*, Optica Applicata **40**(2), 2010, pp. 459–469.

Received February 24, 2017